Dynamic Fracture Analysis of Unsteady Rapid Crack Propagation

新川, 和夫
Research Institute for Applied Mechanics Kyushu University

MADA, Toshia
Research Institute for Applied Mechanics Kyushu University

TAKAHASHI, Kiyoshi
Research Institute for Applied Mechanics Kyushu University

Dynamic Fracture Analysis of Unsteady Rapid Crack Propagation

Kazuo ARAKAWA, Toshio MADA, and Kiyoshi TAKAHASHI

E-mail of corresponding author: k.arakaw@riam.kyushu-u.ac.jp
(Received July 30, 2001)

Abstract

Dynamic crack propagation in PMMA was studied using the method of caustics in combination with a Cranz-Schardin type high-speed camera. Four different types of specimen geometries were employed to achieve the crack acceleration, deceleration and re-acceleration process in one fracture event. Dynamic stress intensity factor K_{ID} and crack velocity $\dot{a}$ were evaluated in the course of crack propagation to obtain the relationship between K_{ID} and $\dot{a}$. The effect of crack acceleration and deceleration on the K_{ID}-$\dot{a}$ relations was examined.

Key Words : *Dynamic Crack Propagation, Stress Intensity Factor, Crack Velocity, Crack Acceleration, Caustic Method, High-Speed Photography, PMMA*

1. Introduction

Dynamic crack propagation in brittle materials has been investigated using many experimental techniques. Optical methods such as photoelasticity [1-4] and the method of caustics [5-9] have been widely employed for evaluating the state of dynamic stress field around a propagating crack tip, i.e. dynamic stress intensity factor K_{ID}. Crack velocity $\dot{a}$ was also estimated in crack propagation to correlate with K_{ID}. Many experimental studies have been made on the relation between K_{ID} and $\dot{a}$, however, different experiments derived significantly different types of K_{ID}-$\dot{a}$ relationships. Much discussion has taken place on the applicability of the methods employed for K_{ID} evaluation, the definition of the crack tip stresses, the influence of specimen geometries and loading conditions and so forth. In the case of brittle fracture, $\dot{a}$ generally changes with time, resulting in crack acceleration or deceleration according to the stress distribution in the specimen. The crack acceleration is an important parameter to understand the behavior of dynamic crack propagation, however, quantitative discussion on the effect of the crack acceleration and deceleration on K_{ID} has been limited.

The purpose of the present work was to study this problem in more detail using the method of caustics in combination with a Cranz-Schardin type high-speed camera [10-11]. Four different types of specimen geometries were employed so that cracks could undergo acceleration, deceleration and re-acceleration stages in one fracture process. Dynamic stress intensity factor K_{ID} and crack velocity $\dot{a}$ were evaluated in the course of crack propagation. The K_{ID}-$\dot{a}$ relations were determined for the stages of acceleration, deceleration and/or re-acceleration. Attention was focussed particularly on the effect of the crack acceleration and deceleration on the K_{ID}-$\dot{a}$ relations.

2. Experimental Procedure

Specimen geometries used in this experiment are illustrated in Fig. 1, where (a) represents a single-edge-notched (SEN) specimen, (b) a uniaxially pin-loaded specimen, (c) a biaxially pin-loaded specimen and (d) a SEN with two circular holes specimen. These four types of specimens were selected to obtain the different behaviors of dynamic crack propagation. The specimens were fabricated from a 5mm-thick sheet of PMMA (Acrylite S-001). A sharp precrack was generated by momentum-controlled chisel-impact into a pre-machined saw-cut on the specimen edge.

All specimens were tested under a displacement controlled condition using a tensile testing machine. Tests

---

*1 Research Institute for Applied Mechanics, Kyushu University

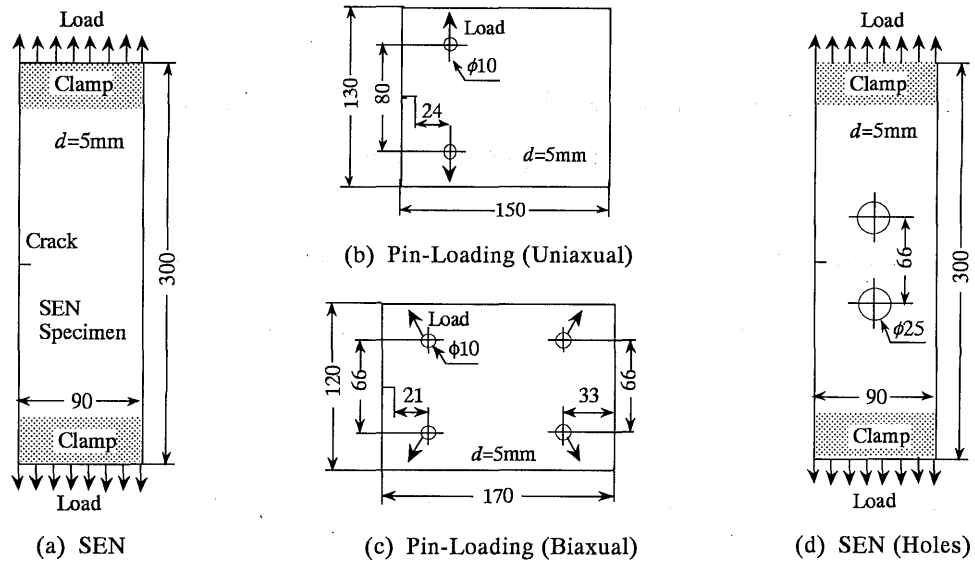(a) SEN (b) Pin-Loading (Uniaxual) (c) Pin-Loading (Biaxual) (d) SEN (Holes)

Fig. 1 Specimen geometries and loading methods

were performed at room temperature and at a constant crosshead speed of 1mm/min. Figure 2 shows the Cranz-Schardin type high-speed camera with 30 spark gaps which permitted bifocal photography [10-11]. The lens box contained a half mirror as illustrated in Fig. 3. The mirror was placed at an angle of 45° with regard to the impinging light rays so that it partly split the rays in a rectangular direction. One focal distance was selected for specimen-focussed images and the other for caustic images.

3. Evaluation of K_{ID} and $\dot{a}$

Figure 4 shows examples of high-speed photographs taken with a SEN specimen, where series (a) represents the specimen-focussed images and (b) the corresponding caustic patterns. As seen, size of the caustic changed with growing crack length. The stress intensity factor K_{ID} was determined from the following equation:

$$K_{ID} = (2\sqrt{2\pi}/3z_0 dc\eta^{3/2})(\phi/3.17)^{5/2} \qquad (1)$$

where ϕ is the caustic diameter at a crack tip, z_0 is the distance between the specimen and the image plane, d is the specimen thickness and η is a convergency factor for incident light rays [9].

The values of K_{ID} and crack length a obtained for the four specimens are shown in Figs. 5-8 as a function of time t. The K_{ID} variations for the specimens were different. In the SEN specimen under uniform tensile loading, K_{ID} increased in the initial stage of crack propagation and gradually approached a constant value. The uniaxially pin-loaded specimen exhibited K_{ID} increasing and decreasing behavior. In both the biaxially pin-loaded and SEN (Holes) specimens, there existed three stages of recogniz-

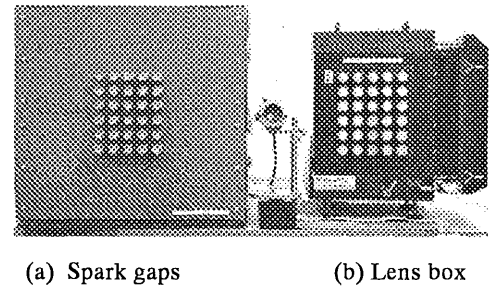(a) Spark gaps (b) Lens box

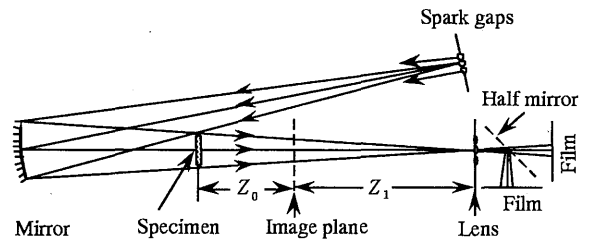Fig. 2 Cranz-Schardin type high-speed camera.

Fig. 3 Optical setup.

able K_{ID} increasing, decreasing and re-increasing regions.

To minimize data scattering in the evaluation of fracture parameters, a data-fitting procedure which was proposed in a previous work [9] was employed; obtained values of K_{ID} and a were expressed as ninth order polynomial of t based on the least-squares method so that they closely fitted their observed values (see Figs. 5-8). Crack velocity $\dot{a}$ was determined from the first time derivatives of the fitted curve $a(t)$. If $\dot{a}$ was determined simply from the first time derivative of increment Δa which was obtained from successive pictures taken on a film, large scatter in $\dot{a}$ was in-
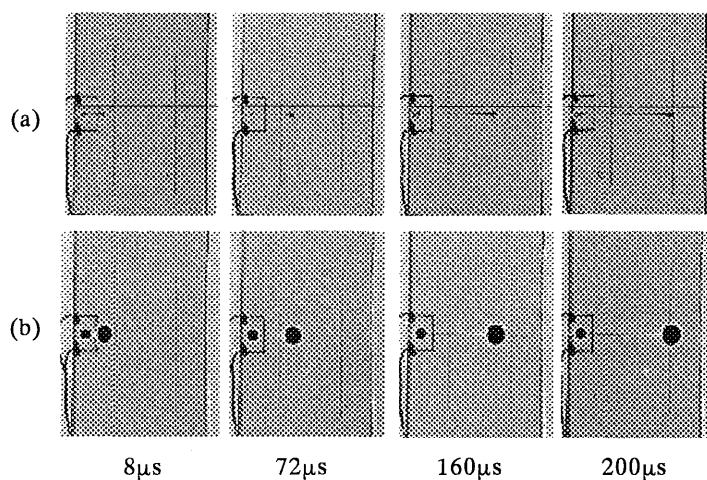
8μs 72μs 160μs 200μs

Fig. 4 Example of dynamic crack propagation in a SEN specimen.
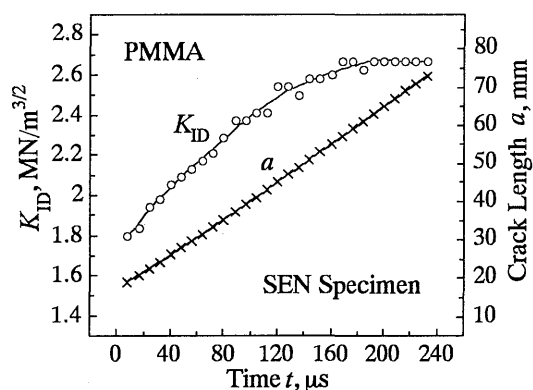(a) specimen-focussed images, (b) caustic patterns

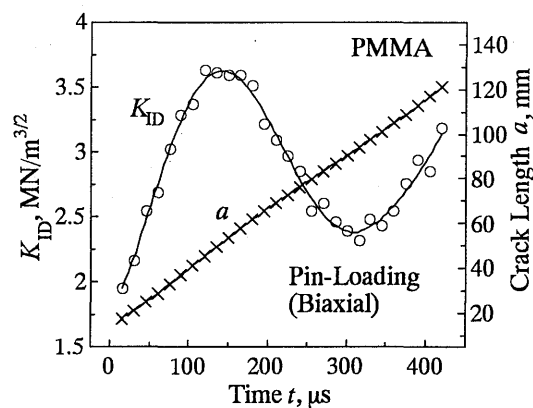Fig. 5 Time variations of K_{ID} and crack length a for
a SEN specimen

Fig. 7 Time variations of K_{ID} and crack length a for
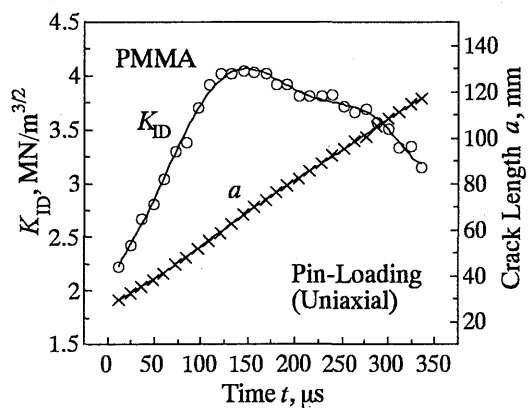a biaxially pin-loaded specimen

Fig. 6 Time variations of K_{ID} and crack length a for
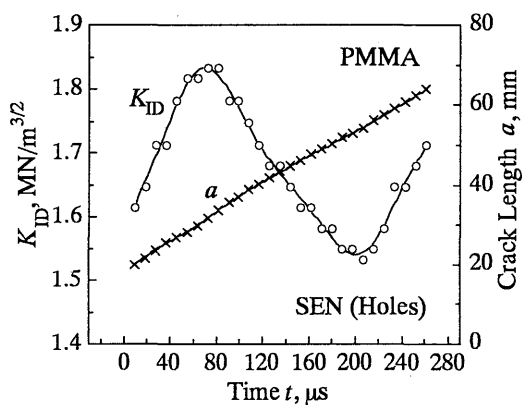a uniaxially pin-loaded specimen

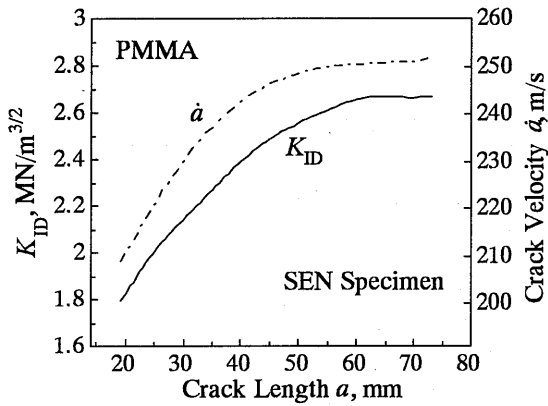Fig. 8 Time variations of K_{ID} and crack length a for
a SEN with holes specimen

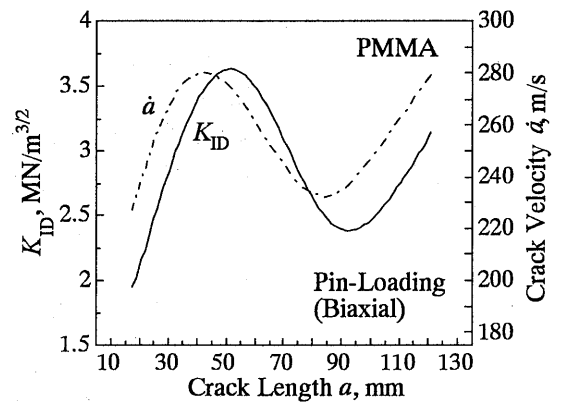Fig. 9　K_{ID} and crack velocity $\dot{a}$ for a SEN specimen

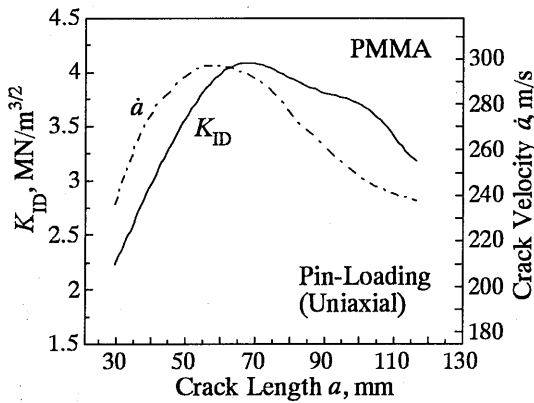Fig. 11　K_{ID} and crack velocity $\dot{a}$ for biaxially pin-loaded specimen

Fig. 10　K_{ID} and crack velocity $\dot{a}$ for a uniaxially pin-loaded specimen
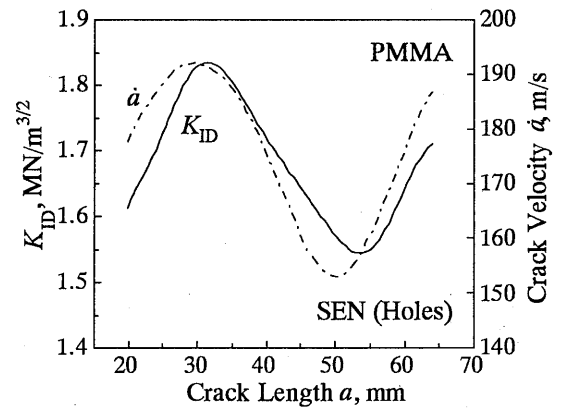

Fig. 12　K_{ID} and crack velocity $\dot{a}$ for a SEN with holes specimen

evitably caused primarily by errors arising from visual identification of the crack tip position on film. Thus, the data-fitting procedure employed enabled us to determine crack velocity accurately.

4. K_{ID} and $\dot{a}$　Relationships

Figures 9-12 show values of K_{ID} and $\dot{a}$ as a function of crack length a. There are several interesting points in their relations. First, the change in $\dot{a}$ was qualitatively in accord with the one in K_{ID}. Second, $\dot{a}$ rose earlier than K_{ID} associated with a. Finally, K_{ID} for a constant $\dot{a}$ was larger when the crack was decelerated than when it was accelerated (see Figs. 10-12). Similar results were also obtained by the authors for epoxy and Homalite-100 specimens[12-15].

To study the effect of the crack acceleration and deceleration, the values of K_{ID} were expressed as a function of $\dot{a}$. Figures 13-16 show $K_{ID}(\dot{a})$ curves, where arrows indicate the direction of progress of the fracture. The open circles represent the acceleration-free points ($\ddot{a}=0$) obtained from the maximum and minimum velocity posi-

tions. There are several interesting points in the K_{ID}-$\dot{a}$ relations. First, $K_{ID}(\dot{a})$ for the SEN specimen only exhibited the increasing process so that it gradually approached a constant value. Second, distinct crack acceleration ($\ddot{a}>0$) and deceleration ($\ddot{a}<0$) can be seen in the uniaxially pin-loaded specimen. Finally, in both the biaxially pin-loaded and SEN (Holes) specimens, three stages of distinct crack acceleration ($\ddot{a}>0$), deceleration ($\ddot{a}<0$) and re-acceleration ($\ddot{a}>0$) can be seen in one fracture process. Although $K_{ID}(\dot{a})$ is shown to increase with $\dot{a}$, it should be noted that their relation was not unique. For a constant $\dot{a}$, the decelerating crack had a larger value of K_{ID} than the accelerating or re-accelerating one. Such was also the case with other specimens tested.

The authors have suggested that K_{ID} was expressed as two parametric functions of $\dot{a}$ and $\ddot{a}$, i.e. $K_{ID}(\dot{a}, \ddot{a})$, and that $K_{ID}(\dot{a}, \ddot{a}=\text{constant})$ was uniquely related to $\dot{a}$ [9,12,13]. This was examined using the obtained results. Figure 17 shows the $K_{ID}(\dot{a})$ curves determined for the four specimens. The dotted curve of $K_{ID}(\dot{a}, \ddot{a}=0)$ connecting the acceleration free points can separate the acceleration ($\ddot{a}>0$) and decel-
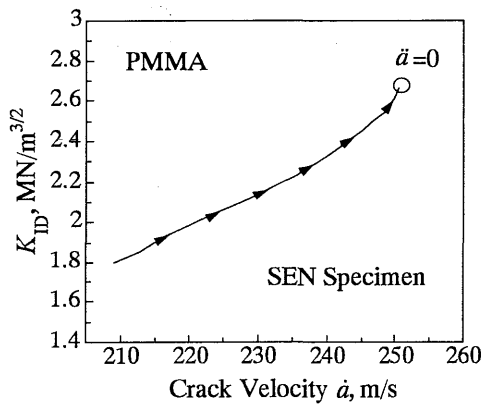
Fig. 13 K_{ID}-$\dot{a}$ relation for a SEN specimen
under unifrom tensile loading
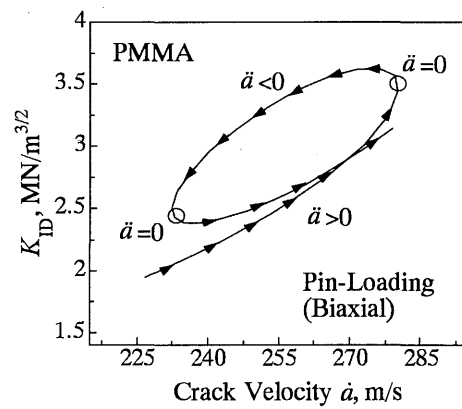
Fig. 15 K_{ID}-$\dot{a}$ relation for a biaxially
pin-loaded specimen
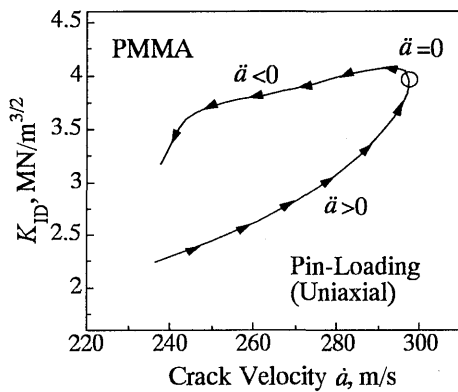
Fig. 14 K_{ID}-$\dot{a}$ relation for a uniaxially
pin-loaded specimen
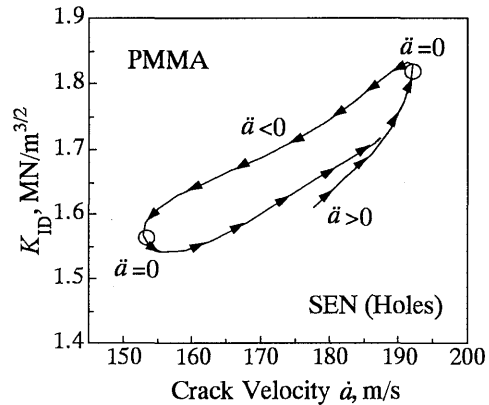
Fig. 16 K_{ID}-$\dot{a}$ relation for a SEN with
holes specimen

eration ($\ddot{a}<0$) area in the K_{ID}-$\dot{a}$ diagram. As seen, $K_{ID}(\dot{a})$ for a constant $\dot{a}$ had a larger value when the crack was decelerated than when it was accelerated, i.e. $K_{ID}(\dot{a}, \ddot{a}<0) > K_{ID}(\dot{a}, \ddot{a}>0)$. It should be noted that $K_{ID}(\dot{a}, \ddot{a}=0)$ can be uniquely related to $\dot{a}$ as suggested in previous studies [9-13]. Hence, this clearly appears to indicate that $K_{ID}(\dot{a}, \ddot{a}=0)$ can be the material property, while the time variations of K_{ID} and $\dot{a}$ were strongly influenced by specimen geometries and loading methods as shown in Figs 9-12.

5. Conclusions

Dynamic crack propagation in PMMA was studied using the method of caustics and a Cranz-Schardin high-speed camera. Four different types of specimen geometries were employed to achieve the crack acceleration, deceleration and re-acceleration process in one fracture event. Dynamic stress intensity factor K_{ID} and crack velocity $\dot{a}$ were evaluated, and the following findings were obtained:

(1) The variations of K_{ID} and $\dot{a}$ were strongly influenced
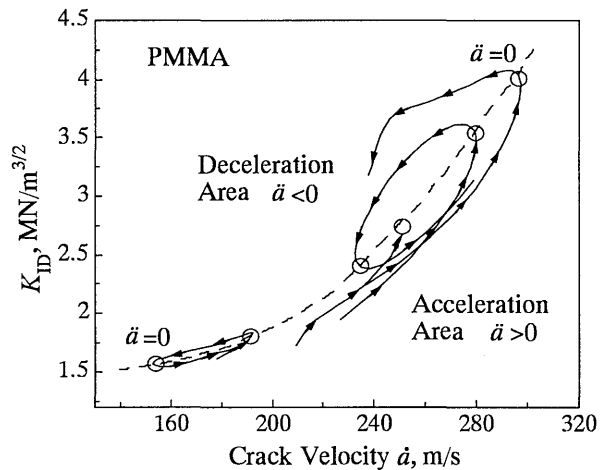
Fig. 17 K_{ID}-$\dot{a}$ curves for the four different types
of PMMA specimens

by the specimen geometries and loading methods.

(2) $\dot{a}$ change was qualitatively in accord with the one in K_{ID}.

(3) K_{ID} for a constant $\dot{a}$ was larger when the crack was

decelerated than when it was accelerated or re-accelerated.

(4) K_{ID} for acceleration-free can be uniquely related to $\dot{a}$.

References

1) J.W. Dally, W.L. Fourney and G.R. Irwin (1985) "On the uniqueness of the stress intensity factor - crack velocity relationship", *Int. J. Fracture*, **27**, 159-168.

2) A.S. Kobayashi, M. Ramulu, M.S. Dadkhah, K.-H. Yang and B.S.J. Kang (1986) "Dynamic fracture toughness" *Int. J. Fracture*, **30**, 275-285.

3) A. Shukla and H. Nigam (1986) "A note on the stress intensity factor and crack velocity relationship for Homalite 100" *Engng Fracture Mech.*, **25**, 91-102.

4) J.W. Dally, R.K. Agarwal and R.J. Sanford (1990) "A study of hysteresis in the K_{ID}-$\dot{a}$ relation" *Exp. Mech.*, **30**, 177-183.

5) J.F. Kalthoff (1983) "On some current problems in experimental fracture dynamics" In W.G.Knauss (ed.), *Workshop on Dynamic Fracture,* California Institute of Technology,Pasadena,11-35.

6) W.G. Knauss and K. Ravi-Chandar (1985) "Some basic problems in stress wave dominatedfracture" *Int. J. Fracture*, **27**, 127-143.

7) T. Nishioka, T. Murakami, H. Uchiyama, K.Sakakura and H. Kittaka (1991) "Specimen size effects on dynamic crack propagation and arrest in DCB specimens" *Engng Fracture Mech.*, **39**, 757-767.

8) A.J. Rosakis (1993) "Two optical techniques sensitive to gradients of optical path difference: the method of caustics and the coherent gradient sensor (CGS)" In J.S. Epstein (ed.), *Experimental Techniques in Fracture*, VCH Publishers, 327-425.

9) K. Takahashi and K. Arakawa (1987) "Dependence of crack acceleration on the dynamic stress - intensity factor in polymers" *Exp. Mech.,* **27**,195-200.

10) K. Arakawa and K. Takahashi (1991) "Branching of a fast crack in polymers" *Int. J. Fracture*, **48**, 245-259.

11) K. Takahashi and T. Mada (1993) "Dual-focus high-speed photography and its application to fracture and impact studies" In J.M. Dewey and R.G. Racca (eds.), *20th International Congress on High-Speed Photography and Photonics,* SPIE 1802, 901-909.

12) K. Arakawa and K. Takahashi (1991) "Relationships between fracture parameters and fracture surface roughness of brittle polymers" *Int. J. Fracture*, **48**, 103-114.

13) K. Arakawa, D. Nagoh and K. Takahashi (1997) "Crack velocity and acceleration effects on the dynamic stress intensity factor in polymers" *Int. J. Fracture*, **83**, 305-313.

14) K. Takahashi, M. Kido and K. Arakawa (1998) "Fracture roughness evolution during mode I dynamic crack propagation in brittle materials" *Int. J. Fracture*, **90**, 119-131.

15) K. Arakawa, D. Nagoh and K. Takahashi (1999) "Dynamic Crack propagation and unloading behavior of brittle polymers" *Int. J. Fracture*, **96**, 345-358.